
# Contribution of cylindrical shear resistance to seismic response of helical piles

Gustavo Padros[1] and Richard Schmidt[2]

[1] Senior Geotechnical Engineer, IPE Engineering Ltd, Edmonton, AB, Canada.
[2] Senior Engineer, Almita Piling Inc, Ponoka, AB, Canada.

## ABSTRACT

The propagation of dilatational and shear waves through soils produce detrimental effects that need to be considered in the design of deep foundations. Additional soil shear stresses are produced due to the propagation of shear waves and due to the increase in pile loads caused by the overturning moment acting on the superstructure. Furthermore, the dilatational wave produces an increase in pore pressure, which leads to a decrease in the effective stress and consequently a decrease in the soil shear strength.

Helical piles manufactured with multiple helices spaced up to about 3 times the helix diameter derive their compressive resistance from shaft friction, cylindrical shear resistance (CSR) and end bearing. Given that the displacement to fully mobilize end bearing is relatively large, helical piles subjected to seismic loading must rely on cylindrical shear to resist the increment in compressive load if large settlements are to be avoided. Understanding CSR thus becomes of paramount importance in the design of helical piles subject to seismic loading. A methodology based on Zeevaert's theory is presented in the present paper that allows designing CSR for seismic loads.

Keywords: helical piles, soil shear strength, dilatational waves, shear waves.

## INTRODUCTION

Seismic waves produced by earthquakes propagate from the focus through deep rock towards the earth surface. Two types of seismic waves are developed when seismic waves travelling from the zone of generation reach the firm ground - soil deposits interphase. These are the dilatational waves and the shear waves, which travel at different speeds and reach the ground surface at different times. These seismic waves are important for the design of deep foundations. The surface (Rayleigh) wave is a third type of seismic wave, which is developed once the other waves reach the surface and is not considered herein.

The dilatational waves travel faster than the shear waves and are the first to arrive at the place of observation. The translation of dilatational waves requires changes in soil volume. Therefore, in saturated soils they produce high pore water pressures, although in saturated soils the displacements they cause are small. On the contrary, shear waves do not produce volume changes in the soil during their propagation. However, high shear distortions may be induced and shear stresses greater than the soil shear strength could be developed.

Helical piles are able to develop considerable compressive and uplift resistances, which make them viable as a deep foundation alternative in earthquake regions. The pile compressive resistance comprises shaft friction and end bearing, and if the helical pile has been manufactured with several helices installed relatively close (typically spaced apart not more than 3 times the helix diameter), a cylindrical shear resistance (CSR) is developed between the uppermost and lowermost helices, which also contributes to the compressive resistance of the pile. Furthermore, the uplift resistance of the helical pile comprises shaft friction and upward bearing of the uppermost helix. Piles manufactured with multiple helices adequately spaced also develop cylindrical shear resistance in uplift loading.

The Canadian Foundation Engineering Manual [1] includes design equations to compute the compressive and uplift resistance of helical piles applying Limit States Design, using Ultimate Limit States (ULS) and Service Limit States (SLS). Those equations have given adequate results, provided that the soil shear strength parameters are accurate. However, in the case of earthquake conditions, additional soil shear stresses have to be considered due to the presence of seismic shear waves and due to the increase in pile loads caused by the overturning moment acting on the superstructure. Furthermore, the dilatational wave produces an increase in pore pressure, which leads to a decrease in the effective stress and consequently a decrease in the soil shear strength. On this basis, the design of helical piles in earthquake regions requires analyzing the combined effects of an increase in soil shear stress (due to shear wave action plus greater pile loads due to the structure overturning moment) and a decrease in soil shear strength (due to an increase in pore pressure).

A well designed helical pile subject to compressive load will develop a relatively small vertical displacement when loaded to service conditions, typically less than 6 mm. At this load level and vertical displacement, the pile may have developed full mobilization of shaft friction, partial mobilization of CSR and small mobilization of end bearing. Given that the displacement to fully mobilize end bearing is relatively large and that no more shaft friction is available, helical piles subject to seismic loading must rely on cylindrical shear to resist the increment in compressive load if large settlements want to be avoided. Understanding of CSR thus becomes of great importance in the design of helical piles subject to seismic loading.

The objectives of the present paper are: (1) Discuss the influence of the dilatational and seismic waves on the cylindrical shear resistance of helical piles; (2) Apply Zeevaert's theory [2-5] to determine the decrease in soil shear strength and the increase in the soil shear stress due to earthquakes; and (3) Compute the CSR developed when seismic loads are present.

## INCREMENT IN PORE WATER PRESSURE DUE TO DILATATIONAL WAVE

The increment in pore water pressure due to dilatational waves has been studied by Zeevaert [2], who developed a methodology based on the following rationale:

(a) The dilatational wave propagates from firm ground to the surface according to the following equation:

$$v_d{}^2 \, \frac{\delta^2 w}{\delta z^2} = \frac{\delta^2 w}{\delta t^2} \qquad (1)$$

where $w$ is the vertical displacement and $v_d$ is the dilatational wave velocity

(b) From theory of elasticity we know that the soil pressure $\sigma_z$ is given by:

$$\sigma_z = E_c \, \frac{\delta w}{\delta z} \qquad (2)$$

where $E_c$ is the dynamic soil modulus, given by :

$$E_c = 2\,(1+\nu)\mu \qquad (3)$$

where $\nu$ is the Poisson ratio and $\mu$ is the shear modulus, equal to :

$$\mu = v_d{}^2 \, \rho \, \frac{(1-2\nu)}{2\,(1-\nu)} \qquad (4)$$

where $\rho$ is the unit mass of the soil, equal to the soil unit weight divided by the gravitational acceleration.

(c) Zeevaert [2] solves equation (2) as:

$$\sigma_z = -E_c \, w_o \, \frac{\pi}{2D} \sin\!\left(\frac{\pi}{2}\,\frac{z}{D}\right) \qquad (5)$$

where $w_o$ is the vertical displacement amplitude, given by :

$$w_o = \frac{4D^2}{\pi^2}\,\frac{\rho}{E_c}\,G_{av} \qquad (6)$$

where $G_{av}$ is the maximum vertical ground surface acceleration.

(d) Substituting equations (3), (4) and (6) in (5) we obtain:

$$\sigma_z = -\left(\frac{2}{\pi}\,G_{av}\,D\,\rho\right)\sin\!\left(\frac{\pi}{2}\,\frac{z}{D}\right) \qquad (5)$$

(e) Considering that during the earthquake, the increase in soil pressure in the saturated soil sediment occurs at constant volume, requiring the decrease in soil effective stress to be equal to increase in pore water pressure, $\sigma_z = -u_z$ , hence:

$$u_z = \left(\frac{2}{\pi}\,G_{av}\,D\,\rho\right)\sin\!\left(\frac{\pi}{2}\,\frac{z}{D}\right) \qquad (6)$$

Equation (6) can be used to determine the increment in pore water pressure caused by the dilatational shear wave.

## INCREMENT IN SOIL SHEAR STRESS DUE TO SHEAR WAVE

The shear waves propagate from the firm ground interphase into the soil deposits, producing important shear distortions in the soil mass, causing an increase in shear stress which is additive to the static shear stress acting on the soil prior to the earthquake (Figures 1 and 2). Furthermore, the shear waves are slower than the dilatational waves and hence arrive later at the place of observation. On this basis, it is considered that the pore pressure caused by the dilatational wave has already increased by the time the shear waves arrive at the foundation.

The increment in soil shear stress due to shear waves has been studied by Zeevaert [2-5], who presented the following methodology for the computation of the shear stress:

(a) The time required by the shear wave to travel through the full soil deposit, from firm ground to the surface, is equal to ¼ the soil dominant period $T$, therefore:

$$\frac{1}{4}T = \frac{D}{v_s} \qquad (7)$$

where $D$ is the depth between the ground surface and the firm ground, and $v_s$ is the shear wave velocity. In stratified soil deposits, Equation (7) is modified as follows:

$$\frac{1}{4}T = \Sigma_{i=1}^{n} \frac{d_i}{(v_s)_i} \qquad (8)$$

(b) The shear wave velocity is a function of the dynamic shear modulus $\mu$ as follows :

$$v_s^{\,2} = \frac{\mu}{\rho} \qquad (9)$$

(c) The dynamic shear modulus $\mu$ can be determined in the field from seismic cone penetration tests, crosshole seismic surveys, downhole seismic surveys, or other field tests. Alternatively, it may be determined through laboratory tests in soil samples, which may include resonant column tests, free torsion pendulum tests or other.

(d) The shear wave propagates from firm ground to the surface according to the following equation:

$$v_s^{\,2} \frac{\delta^2 u}{\delta z^{\,2}} = \frac{\delta^2 u}{\delta t^{\,2}} \qquad (10)$$

where $u$ is the vertical displacement. Since the values of $\mu, \rho$ and consequently $v_s$ change for every soil layer, Zeevaert [3], developed an integration method to solve Equation (10) as follows:

(e) The algorithms for the computation of the maximum horizontal displacements $\delta_i$ and the corresponding shear stresses $\tau_i$ in each soil layer for the ground motion induced by the shear waves are given by:

$$\delta_{i+1} = A_i\, \delta_i - B_i\, \tau_i \qquad (11)$$

$$\tau_{i+1} = C_i\, (\delta_i + \delta_{i+1}) + \tau_i \qquad (12)$$

where the coefficients have the following values :

$$A_i = \frac{1 - N_i}{1 + N_i} \qquad (13)$$

$$B_i = \frac{1}{1 + N_i} \left(\frac{\delta_i}{\mu_i}\right) \qquad (14)$$

$$C_i = \frac{1}{2} \rho\ \delta_i\ \omega_n^2 \qquad (15)$$

$$N_i = \frac{\rho\, \delta_i^2\, \omega_n^2}{4\mu_i} \qquad (16)$$

and $\omega_n$ is the angular frequency of the soil mass, which initially can be computed from the soil period as follows:

$$\omega_n = \frac{2\pi}{T} \qquad (17)$$

(f) The calculations start by computing a ground surface displacement $\delta_1$ equal to :

$$\delta_1 = \frac{G_{av}}{\omega_n} \quad (18)$$

and assume that the increment in shear stress at the ground surface due to the shear wave is zero ( $\tau_1 = 0$).

(g) Subsequently equations (11) and (12) are computed for each soil layer starting from the ground surface, using the coefficients in equations (13) to (16).

(h) When the calculations reach firm ground, the horizontal displacement computed should be zero. If this is not the case, the angular frequency initially assumed in equation (17) should be corrected and a new iteration undertaken from the ground surface to the firm ground.

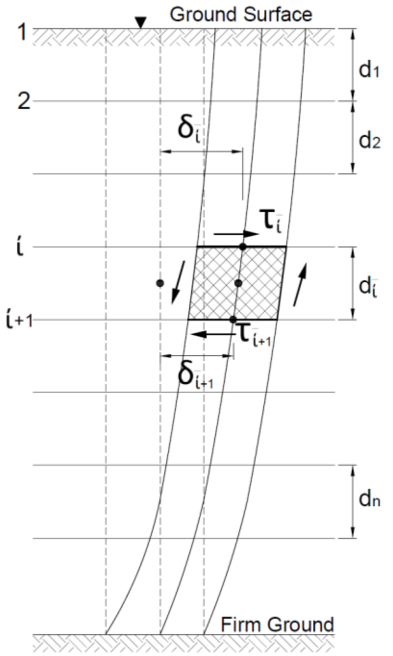


Figure 1. Shear stress due to shear wave.

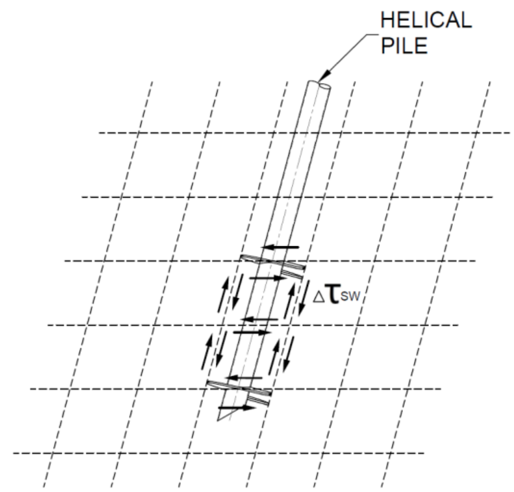


Figure 2. Shear stress on helical pile CSR due to shear wave

## INCREMENT IN SOIL SHEAR STRESS DUE TO OVERTURNING MOMENT TRANSFERRED TO PILES SUPPORTING RIGID STRUCTURES

The present Section considers a rigid superstructure on a rigid mat or box foundation supported by helical piles, as shown in Figure 3. It is assumed that the underside of the foundation slab is not in contact with the soil underneath, therefore the vertical loads acting on the structure are directly transferred to the helical piles.

As the result of an earthquake, a horizontal seismic shear force $V_M$ will be produced on a structure, acting on its centre of mass located on a height $h_M$, producing a seismic overturning moment $O_{TM}$ as shown in Figure 5. The overturning moment will produce dynamic loads on the piles, which will be additional to the static loads previously acting.

The procedure to determine the horizontal seismic shear force acting on the structure is included in Building Codes. The present Section does not summarize any procedure, rather it is assumed that the overturning moment has already been computed.

The determination of the dynamic loads transferred to the piles requires undertaking soil-structure interaction calculations. For the purposes of the present paper, a simple approach is presented, consisting on computing the increase in pile load $\Delta P_i$ due to earthquake using the following equation:

$$\Delta P_i = \frac{M_y\, x}{\Sigma\, x^2} + \frac{M_x\, y}{\Sigma\, y^2} \quad (19)$$

where $M_y$ and $M_x$ the factored overturning moments due to earthquake loading and $x$ and $y$ are the distances of the piles to the center of gravity of the foundation.

Once the decrease in soil shear strength and the increase in the soil shear stress due to earthquakes has been determined, the next step is to carry out laboratory tests to find out if the soil has adequate resistance to develop the necessary CSR to support the seismic loads. Triaxial cyclic tests or direct shear tests (cyclic or conventional) may be carried out. Direct shear tests are particularly desirable since the distortion produced in the soil sample during the test resembles the distortion of the soil between the helices when a helical pile is loaded in the field. The use of direct shear test results to understand the development of CSR under static loading has been applied by Padros [6-7].

On this basis, the methodology presented in previous Sections is shown in Figure 4, where $\Delta\tau_{sw}$ is the additional soil shear stress due to the shear waves and $\Delta\tau_{OTM}$ is the additional soil shear stress due the increase in pile loads caused by the overturning moment acting on the superstructure. The confinement effective stress between the helices is $\sigma_c$. Furthermore, the dilatational wave produces an increase in pore pressure, which leads to a decrease in the confinement effective stress $\Delta\sigma_c$ . Therefore, the direct shear test is carried out applying a compressive effective stress $\sigma_c - \Delta\sigma_c$ . In that test, the total increase in shear stress due to sesimic loads is $\Delta\tau_{sw} + \Delta\tau_{OTM}$, which has to be compared with the maximum shear resistance of the soil.

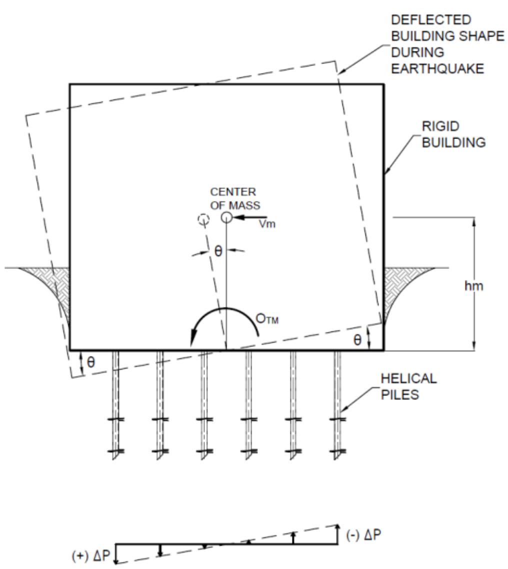


Figure 3. Pile loads due to overturning moment

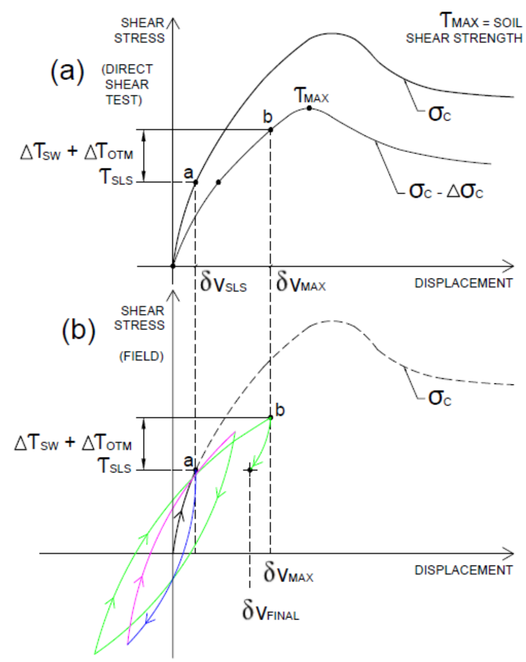


Figure 4. Shear stress increase acting on CSR

## EXAMPLE OF CSR COMPUTATION CONSIDERING SEISMIC CONDITIONS

### General

An example is presented to illustrate the computation of the CSR of a helical pile subject to seismic load. The example considers a rigid superstructure on a rigid shallow foundation supported by helical piles, as shown in Figure 5. The ULS and SLS static compressive loads on each pile are 45 ton and 32 ton, respectively. The overturning moments in the X and Y directions due to the horizontal seismic shear forces are 1,000 ton·m and 600 ton·m, respectively. A maximum vertical ground surface acceleration $G_{av}$ of 1 m/sec$^2$ is considered. The subsurface conditions correspond to a stratified deposit comprising granular and cohesive soil layers extending to 24 m depth, where firm ground is encountered. The groundwater level is located at the ground surface. The parameters for each soil layer are presented in Table 1. The shear strength parameters of the soil layers are also included in Table 1 (undrained shear resistance Cu and angle of internal friction φ.

All helical piles have the same size, consisting of a 273 mm shaft diameter and two helices 762 mm diameter, located at 12.24 m and 13.76 m depth (therefore the helix spacing is 1.524 m). The piles head is at 2 m depth and is pinned to the slab. The piles length is 12 m, extending from 2 m to 14 m depth. Based on CFEM, the unfactored compressive resistance of the helical pile is 210 ton, comprising a shaft friction of 20 ton, CSR of 30 ton and an end bearing of 160 ton. The factored geotechnical resistance is hence 84 ton, adequate to support the ULS compressive load of 45 ton.

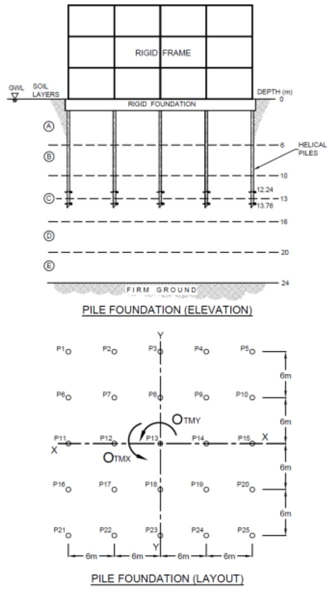


Figure 5. Building and soils conditions used in example

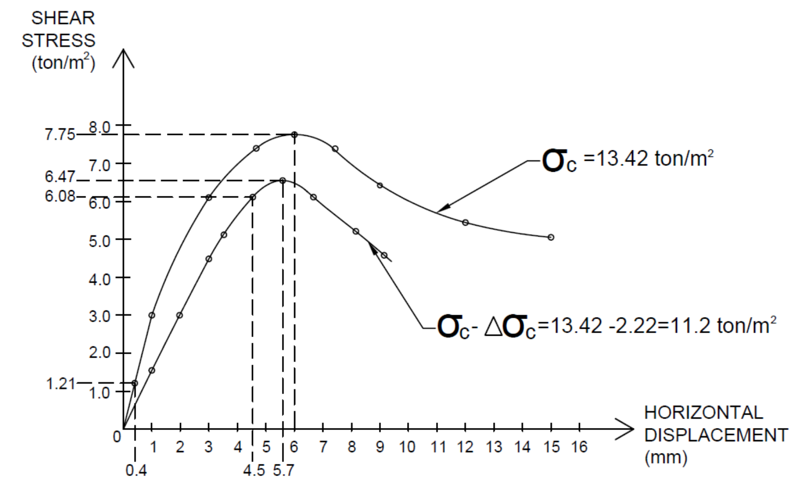


Figure 6. Shear stress computation based on the results of a direct shear test.

*Table 1. Soil Properties and Parameters.*

| Layer | Depth (m) | Soil Type | Unit Weight (ton/m$^3$) | Vs (m/sec) | Cu (ton/m$^2$) | φ (deg) |
|---|---|---|---|---|---|---|
| A | 0 – 6 | Sand | 1.85 | 90 | 0 | 28 |
| B | 6 – 10 | Clay | 1.80 | 50 | 15 | 0 |
| C | 10 – 16 | Sand | 1.90 | 100 | 0 | 30 |
| D | 16 – 20 | Clay | 1.95 | 70 | 10 | 0 |
| E | 20 – 24 | Sand | 2.00 | 120 | 0 | 32 |

**Considerations**

The computation of the CSR is based on the following considerations:

(a) Rigid superstructure on a rigid shallow foundation.
(b) The vertical loads acting on the structure are directly transferred to the helical piles.
(c) The increase in pore pressure produced by the dilatational waves, which arrive first to the deep foundation location, is still present once the shear waves arrive.
(d) The increase in soil shear stress (due to shear wave action and due to greater pile loads caused by the structure overturning moment) occurs at the same time the soil shear strength decreases (due to an increase in pore pressure).
(e) Soil is saturated.
(f) The SLS load acting on each pile is 32 ton. Considering that a small vertical pile displacement has developed under service conditions, sufficient to fully mobilize the shaft friction but negligible mobilization of end bearing has occurred, then the CSR mobilized under SLS conditions is about 32 ton – 20 ton = 12 ton. Therefore, the CSR available to resist the increase in load due seismic forces is about 30 ton – 12 ton = 18 ton.
(g) The vertical effective stress at mid height between the helices (13 m depth) under static conditions is 11 ton/m$^2$ + 4.84 ton/m$^2$ = 15.84 ton/m$^2$, where 11 ton/m$^2$ is the vertical stress prior to pile installation and 4.84 ton/m$^2$ is the increase in vertical stress caused by the loaded pile under static conditions.
(h) The confining effective stress increases in the proximity of the pile after this has been installed. On this basis, the confining effective stress at mid height between the helices under static conditions is considered equal to about 1.2 times the vertical effective stress (therefore equal to 13.4 ton/m$^2$).
(i) The shear stress acting in the soil on vertical planes between the helices under static pile loading conditions was calculated as (15.84 ton/m$^2$ – 13.4 ton/m$^2$)/2 = 1.21 ton/m$^2$
(j) The CSR alone will have to resist the increase in pile load due to earthquake.

**CSR computations**

(a) Initial calculations

The shear modulus and the ratios $\frac{d_i}{(v_s)_i}$ are computed in Table 2. From that Table and equations (8), (17) and (18) we obtain the soil period T = 1.1 sec, angular frequency $\omega_n$ = 5.7 sec$^{-1}$ and ground surface displacement $\delta_1$ = 0.03 m.

*Table 2. Calculation of Soil Mass, Shear Modulus and Soil Period.*

| Layer | Thickness $d_i$ | Soil Mass ρ | Shear Modulus μ | $d_i/(Vs)_i$ |
|---|---|---|---|---|
| A | 6 | 1.85 | 1,525 | 0.044 |
| B | 4 | 1.80 | 450 | 0.080 |
| C | 6 | 1.90 | 1,950 | 0.060 |
| D | 4 | 1.95 | 975 | 0.057 |
| E | 4 | 2.00 | 2,950 | 0.033 |

(b) Increment in pore pressure caused by dilatational wave

The increment in pore water pressure is computed from equation (6), considering an average unit mass of the soil $\rho$ equal to 0.193 ton·sec/m$^4$. Substituting the parameters in Equation (6), we obtain the increment in pore water pressure caused by the dilatational wave, computed given by the equation below. The results are summarized in Table 3.

$$u_z = [\frac{2}{\pi}\left(1\ \frac{m}{sec^2}\right)\ 24\ m\ (0.193\ \frac{ton \cdot sec^2}{m^4}]\sin\left(\frac{\pi}{2}\ \frac{z}{24\ m}\right) = 2.95\sin(\frac{\pi\ z}{48})$$

*Table 3. Increment of Pore Water Pressure due to Dilatational Wave.*

| Depth (m) | Uz (ton/m$^2$) | Depth (m) | Uz (ton/m$^2$) | Depth (m) | Uz (ton/m$^2$) |
|---|---|---|---|---|---|
| 0 | 0 | 10 | 1.80 | 18 | 2.73 |
| 2 | 0.39 | 12 | 2.09 | 20 | 2.85 |
| 4 | 0.76 | 13 | 2.22 | 22 | 2.92 |
| 6 | 1.13 | 14 | 2.34 | 24 | 2.95 |
| 8 | 1.48 | 16 | 2.55 | | |

(b) Increment in soil shear stress due to shear wave

From equation (18) the ground surface displacement $\delta_1$ = 0.03 m is obtained. The increment in shear stress at the ground surface due to the shear wave is zero ($\tau_1 = 0$). Subsequently, equations (11) and (12) are computed for each soil layer starting from the ground surface, using the coefficients in equations (13) to (16). The results are included in Table 4. The computation results indicate that the horizontal displacement computed at firm ground is zero, which indicates that the angular frequency initially assumed in equation (17) is correct, and there is no need to carry out another iteration.

*Table 4. Computation of Increment of Soil Shear Stress and Displacements due to Shear Wave.*

| Depth | Layer | $d_i$ (m) | ρ | μ | $N_i$ | $A_i$ | $B_i$ | $C_i$ | $\delta_i$ (m) | $\tau_i$ |
|---|---|---|---|---|---|---|---|---|---|---|
| 0 | | | | | | | | | 0.03 | 0 |
| | A | 6 | 1.85 | 1,525 | 36.2 | 0.93 | 3.80 | 18.42 | | |
| 6 | | | | | | | | | 0.029 | 1.10 |
| | B | 4 | 1.80 | 450 | 52.9 | 0.90 | 8.44 | 11.89 | | |
| 10 | | | | | | | | | 0.017 | 1.64 |
| | C | 6 | 1.90 | 1,950 | 7.27 | 0.99 | 1.53 | 9.45 | | |
| 16 | | | | | | | | | 0.011 | 2.17 |
| | D | 4 | 1.95 | 975 | 25.9 | 0.95 | 4.00 | 12.61 | | |
| 20 | | | | | | | | | 0.002 | 2.33 |
| | E | 4 | 2.00 | 2,950 | 8.99 | 0.98 | 1.34 | 13.26 | | |
| 24 | | | | | | | | | 0 | 2.33 |

(c) Increment In soil shear stress due to overturning moment transferred to piles supporting rigid structures

The increase in pile load $\Delta P_i$ due to earthquake is computed using equation (19), considering $\Sigma x^2 = \Sigma y^2 =$ 1,800 m$^2$. The maximum increase will occur in the corner piles (designated No's. 1, 5, 21 and 25 in Figure 5), obtaining $\Delta P_i$ = ±10.7 ton.

Consequently, the increase in the shear stress between the helices due to the increase in pile load $\Delta P_i$ due to earthquake is:

$$\Delta CSR = \frac{\Delta P_i}{\pi\ (D_h)\ (2\ D_h)} = \frac{10.7\ ton}{\pi\ (0.762\ m)\ (2 \cdot 0.762\ m)} = 2.93\ \frac{ton}{m^2}$$

(d) Computation of CSR increase

As mentioned in consideration (i), the initial shear stress acting on the soil under static conditions (on vertical planes between the helices) was assumed to be 1.21 ton/m$^2$. The increase in shear stress due to shear wave action and due to greater pile loads caused by the structure overturning moment should be added to this stress. Based on the calculations undertaken in the previous Sections, the total increase in the shear stress in vertical planes between the helices $\Delta CSR_{TOTAL}$ is equal to:

$$\Delta CSR_{TOTAL} = 1.94\ \frac{ton}{m^2} + \ 2.93\ \frac{ton}{m^2} = \ 4.87\ \frac{ton}{m^2}$$

which produces a cylindrical shear force equal to 17.8 ton, which is basically the CSR that was available to resist the increase in load due seismic forces, as mentioned in consideration (f). The total CSR adding the static plus the dynamic increment is:

$$CSR_{TOTAL} = 1.21\ \frac{ton}{m^2} + \ 4.87\ \frac{ton}{m^2} = \ 6.08\ \frac{ton}{m^2}$$

Furthermore, to determine the effect that the increase in pore pressure has in the shear resistance, direct shear tests can be carried out in representative soil samples retrieved from the soil layers where the helices will be located. In the present example, the results from direct shear tests undertaken in a sample obtained from the sand layer located at 13 m depth are shown in Figure 6. The figure shows the results of the shear stress and displacement developed applying a compressive stress of 13.4 ton/m$^2$. The results of a second test where the increase in pore pressure was deducted from the compressive stress are also shown (i.e, 13.4 ton/m$^2$ – 2.2 ton/m$^2$ = 11.2 ton/m$^2$). Based on the comparison between the two tests it is noticed that the maximum shear resistance decreases from 7.75 ton/m$^2$ to 6.47 ton/m$^2$ due to the increase in pore pressure. Furthermore, it is observed that the CSR has adequate resistance to support the total shear stress acting between the helices (i.e, 6.08 ton/m$^2$ < 6.47 ton/m$^2$). A rough estimate of the transient maximum pile vertical displacement produced during the earthquake, additional to the previous pile vertical displacement under service conditions, may be obtained from Figure 6, equal to about 4.5 mm – 0.4 mm = 4 mm, which is a conservative estimate because the end bearing was neglected.

## CONCLUSIONS

1. Soil deposits subject to seismic loading register an increase in shear stress and a decrease in shear strength. These should be taken into consideration in the design of foundations. Increases in shear stress result from the propagation of seismic shear waves and due to the increase in pile loads caused by the overturning moment acting on the superstructure. Furthermore, the dilatational wave produces an increase in pore pressure, which leads to a decrease in the effective stress and consequently a decrease in the soil shear strength.

2. The increase in shear stress due the shear wave and the decrease in shear strength due to the dilatational wave can be determined applying Zeevaert's theory [2-5]. The methodology to determine the increase in pile loads caused by the seismic overturning moment can be found in Building Codes.

3. Helical piles can be designed to have adequate resistance against seismic loads by a proper design of CSR. This requires leaving additional CSR resistance under SLS conditions such that when the earthquake comes, the CSR still has capacity to take the full seismic load. Small pile displacements should be expected, given that small pile vertical displacements are required to develop CSR.

## ACKNOWLEDGMENT

The Authors are grateful to Hector Ibarra, P. Eng. with Almita Piling Inc. for his help preparing the figures.

## REFERENCES

[1] Canadian Geotechnical Society (2006). *Canadian Foundation Engineering Manual*. Third Edition, Vancouver.
[2] Zeevaert, Leonardo (1991). "Foundation Problems in Earthquake Regions". *Foundation Engineering Handbook.* Fang, H.Y. (Editor). Second Edition. Chapman & Hall, New York.
[3] Zeevaert, Leonardo (1982). *Foundation Engineering for Difficult Subsoil Conditions*. Second Edition. Van Nostrand Reinhold, New York.
[4] Zeevaert, Leonardo (1988). *Seismo-Geodynamics of the Ground Surface*. Editora Internacional, S.A de C.V., Mexico.
[5] Zeevaert, Leonardo (1980). *Interaccion Suelo – Estructura de Cimentacion.* Editorial Limusa. Mexico.
[6] Padros, G. (2013). "Analysis of Cylindrical Shear Resistance of Screw Piles Subjected to Compressive Loads Based on Direct Shear Tests". *1st International Symposium on Helical Piles*. Amherst, Massachusetts.
Padros G. (2013). "Influence of Helix Geometric Configuration on the Cylindrical Shear Resistance of Screw Piles Based on Direct Shear Tests". *Canadian Geotechnical Conference*, Montreal, Quebec.